Design framework for DEM-supported prototyping of grabs including full-scale validation

Schott, Dingena; Mohajeri, Javad; Jovanova, Jovana; Lommen, Stef; de Kluijver, Wilbert

DOI
10.1016/j.jterra.2021.04.003

Publication date
2021

Document Version
Final published version

Published in
Journal of Terramechanics

Journal of Terramechanics 96 (2021) 29–43

Contents lists available at ScienceDirect

Journal of Terramechanics

journal homepage: www.elsevier.com/locate/jterra

Design framework for DEM-supported prototyping of grabs including full-scale validation

Dingena Schott [a,*], Javad Mohajeri [a], Jovana Jovanova [a], Stef Lommen [a], Wilbert de Kluijver [b]

[a] Delft University of Technology, Department of Maritime and Transport Technology, Delft, the Netherlands
[b] Nemag BV, Zierikzee, the Netherlands

ARTICLE INFO

Article history:
Received 2 October 2020
Revised 11 February 2021
Accepted 12 April 2021
Available online 27 May 2021

Keywords:
Grab
DEM-MBD co-simulation
(true) validation
On-site experiments
Design cycle
Industrial-scale

ABSTRACT

The design of machinery for handling granular materials relies mainly on empirical methods and in-house engineering knowledge. This traditional approach provides incremental improvements that are often limited. Advancements in simulation and optimization can offer a promising alternative approach. Most of the research involved in improving or optimizing equipment design does not include the realistic performance of the new prototype and as such it is uncertain that the predicted performance is also guaranteed in practice.

In this study, a design framework for a new generation of machinery handling granular materials, grabs, has been established that includes a full-scale validation step. This has been proven to lead to a breakthrough in equipment design. This design framework uses a co-simulation between Discrete Element Method (DEM) and Multi Body Dynamics (MBD), thus, capturing operational conditions in full-scale. The DEM simulation supported design step integrated as the main step to generate new prototypes. The performance of the prototype is evaluated by conducting full-scale experiments, thus validating the adequacy of the new design as well as the accuracy of the co-simulation. Through this a full design cycle has been fulfilled and a validated model has been achieved that is independent of specific design configurations.

1. Introduction

The traditional design of industrial scale equipment for handling of granular materials such as iron ore, grain and coal in bulk material terminals is typically empirically based. Manufacturers rely on in-house experience and engineering knowledge they have acquired over the years and they can only implement small incremental changes in the design for performance improvement. Granular material handling is a complex process that is heavily influenced by the equipment design itself as well as the material properties, material state and the operational conditions. The operational conditions refer to how a piece of equipment is handled by an operator and environmental variables. Material state includes material properties such as granular size, moisture content and interaction with the equipment. Thus, predicting the performance of new design concepts is challenging, as it requires multiple inputs to match to capture real operational behavior.

The development of Discrete Element Method (DEM) in 1969 [1] has led to nowadays a broad application of DEM models to evaluate equipment design [2–4]. DEM is used to model the granular material behavior in a particular equipment setup. To capture the behavior of the granular material, the material model needs to be calibrated first, which includes inputs like particle size, contact model and materials state. The calibration of the material models is typically done through extracting data from controlled experimental setups for material testing or from on-site tests [5–16]. Calibrated material models can then be used in DEM simulations for performance analyses of different pieces of equipment. The performance analyses give detailed information about the granular material and equipment interaction, which allows the designer to study trends of parametric changes in design variables. The validation is either achieved by small-scale laboratory experiments (e.g. [17–24]) or by full-scale on-site tests (e.g. [2,25–29]). Obermayr et al. [30] validated draft forces on blades in cohesive soil both on a laboratory and full-scale. The validated model can then be used to explore the design space and predict behavior under various operational conditions [19,20,27,31–33].

In reality the granular material equipment interaction is heavily influenced by the change of material state of the granular materials

* Corresponding author.
E-mail addresses: D.L.Schott@tudelft.nl (D. Schott), M.Mohajeri-1@tudelft.nl (J. Mohajeri).

https://doi.org/10.1016/j.jterra.2021.04.003
0022-4898/

and the operational conditions. In [34], a coupled 3D isogeometric and discrete element approach for modeling interactions between structures and granular matters has been presented. A validated robust design approach is necessary to be able to capture the granular material equipment interaction in real operational conditions. A co-simulation between a DEM environment and a multi body dynamics (MBD) simulation environment is necessary, since this allows the equipment to be dynamic and interact with the granular material. The required torques on the winches is a response of the interaction of the grab with the bulk material. The DEM-MBD co-simulation has been explored for improvement of grab performance for wood chips [35]. In this work it was shown that by using coupled MBD-DEM simulations, a significant incremental improvement of the grab design is achieved for use in the unloading of wood chips. However, even in this work was pointed out that it is crucial to carefully measure and calibrate the bulk material. The wood chips are typically soft and elastic and the modulus of elasticity of a bulk material column must be compared with measurements in the simulation. Only in this way a realistic material behavior is assured, which responds to compressions of the bulk material in the grab with realistic forces.

The extent to which the validated material models are valid for the newly designed or virtually optimized configurations is not well described in literature since a demonstration of the performance in full-scale is not included. Likely, this is because the resulting designs are not publicly shared due to confidentiality agreements, whilst from a scientific perspective an essential part of the full design cycle is the proof of concept. Therefore, this research presents the validated DEM-supported design for virtual prototyping of grabs, by testing of full-scale existing design as well as newly built prototype. More specific, the missing link is an evaluation of the full-scale prototype resulting from the DEM supported design process. Filling this gap will prove that the use of developed models is not restricted to existing equipment types, and as such completes the full design cycle. The design framework has been demonstrated with the design of a new generation of grabs for iron ore pellets, and the entire process of the design of a new generation of grabs is documented here.

A typical operational setup for a bulk material handling grab is shown in Fig. 1. The opening and closing of the grab are done from a crane. The crane operator controls the states and position of the grab. The operation is typically performed with one pair of closing cables and one pair of hoisting cables. Two winches are mounted on the crane to operate the hoisting and closing cables respectively.

The grab cycle starts with lowering the opened grab onto the material and the knives cut through the bulk material for initial penetration. Then force is applied in the closing cables and the grab scoops material inside as it is closing. Once the grab is closed, it is pulled up both on the closing and hoisting cables/ropes and then the material is taken to the next point of transport where the grab is opened, and the material is released. The grab performance is estimated mainly on the average unloading capacity (tonne/hour) including both the payload (tonne) and cycle frequency (cycles/hour). The goal is maximum payload in each cycle, however the payload varies based on the bulk material surface and the operational conditions. Also, the overall optimal performance includes that the entire bulk material is transported in minimum overall time, requiring shorter cycle times that is dictated by the operational conditions, not only the design of the grab. Taking into consideration that the grab performance depends on the grab design, the material state and the operational conditions, a design of a new grab traditionally had been only done based on previous experiences and incremental improvements. In the meantime, engineering design has been massively supported with modeling and simulation tools in other industries, resulting in new designs, unimaginable for conventional design techniques. Using DEM-MBD co-simulation, existing grab behavior can be captured and used as a learning tool to achieve breakthrough designs in large scale material handling equipment.

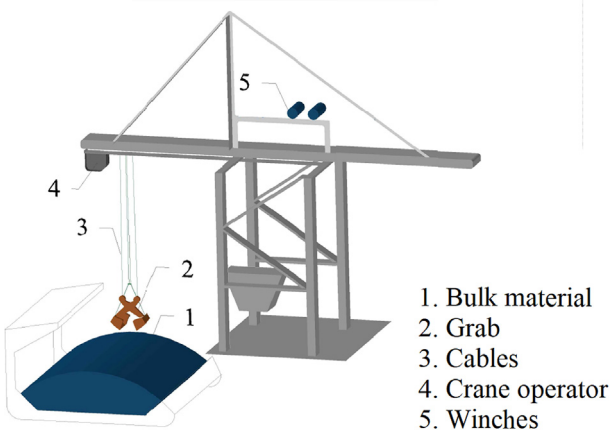

Fig. 1. Operational setup of bulk material handling grab.

This work presents a framework with complete design cycle based on DEM-supported design for virtual prototyping of grabs through validation of the DEM-MBD co-simulation model for an existing grab, then use the validated model to gain insight of design parameters on grab performance. Based on the detailed design parameter analyses a new grab design is engineered and prototyped. Its performance is validated in full size with new design predictions in real operational conditions and the performance matched the expected behavior. This validates the grab independent design framework and can be used for any type of granular material equipment design.

This design framework can be potentially beneficial to all parties concerned in the grab manufacturing process. The client's side (in this case the terminal operator) is not part of the design process. However, with this framework in the future the client's needs can be taken closely into consideration which can lead to highly customized grab designs. The client can specify the material to be handled as well as operational types, and the designer can use the virtual design for sensitivity analyses to discover what kind of grab design meets the client's needs best before the order is placed. The designer can simulate different materials, operational scenarios and grab shapes to discover the optimal grab design. The optimal design is engineered in a specific way to meet the client's customized requirements. The co-simulation results are essential in the definition of KPIs for the grab performance and understand the influence of each design parameter on the grab performance in different operational scenarios and different materials. The co-simulation can support understanding of different design objectives and improve the efforts towards optimal grab design. This design framework creates an opportunity for application-driven design of grabs where the customer's specific requests can lead to custom-made grab design by the manufacturer. This approach is extremely beneficial in the granular equipment handling, because the equipment can be used in different setups as well as for different materials in a variety of setups. Being able to provide the customer with an application-driven design will result in maximum efficiency during equipment lifetime. Moreover, the terminal operators can benefit from this design framework in analyzing the operational grab performances and planning for new ones based on the expected capacity extension. Additional information about the environmental impact and energy consumption can be used in the sustainability evaluation and efficiency planning of a bulk material handling terminal.

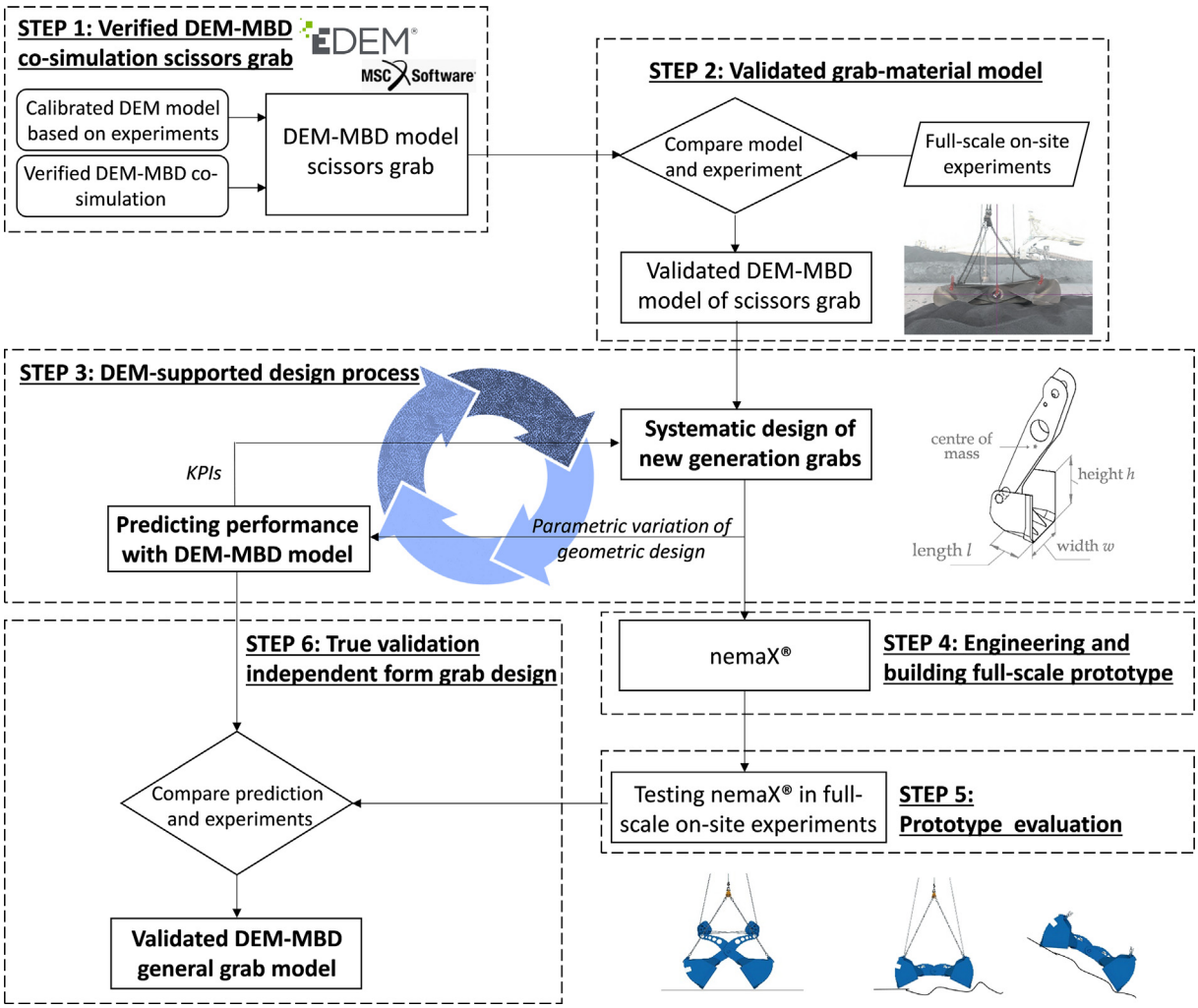

Fig. 2. Design framework and completed design cycle for development of a new generation grabs resulting in a true validation independent form grab design.

Predicting the behavior of a single grab can also be used in optimizing maintenance activities, energy consumption and cost reduction. Such insightful detailed information coming from the co-simulation could be combined with more logistics related simulations. Predicting grab behavior can give a good time estimation on the process of loading and unloading, as well as energy consumption over a period of time. Taking into account the crane input on the grab behavior can give a full estimate of unloading process of a bulk terminal which can be further optimized on a logistics level for maximum port operational efficiency. The design framework is just the first step in the modern grabs' design, and as simulation tools are becoming more powerful, variations in the material state, as well as dynamics optimizations can be introduced. The work presented here is a result of years' long extensive research in granular equipment design and our close collaboration with the industry.

2. Design framework

The design framework developed in this work is a complete design cycle for the development of a new generation grabs resulting in a true validation independent form grab design. The design framework consists of 6 steps that are the core of the design cycle for extended validation of the DEM simulation supported design approach. This framework supports the development of a model that is independent of a specific grab design. The complete DEM supported design cycle for a new grab type is shown in Fig. 2. This design framework is a novel approach in the design of grabs and can be used for generation of new grab shape geometries and closing mechanisms. This approach shifts the entire grab design process from traditional (in-house knowledge; trial and error) to model based (DEM supported design) which is a breakthrough in the grab design.

The steps in the design framework are explained below:

- **Step 1. Verified DEM-MBD co-simulation scissors grab**

The first step in the design framework is developing a model of an existing grab with a specific material. Such a DEM-MBD model allows capturing of the interaction between the material and the grab. Initially, a validation of a multibody model of a scissors grab including sheaves and cables was performed [36]. To operate an empty grab a virtual crane operator was used to open and close the grab. The torques of the winches predicted by the simulation corresponded well with the real operational parameters and therefore the MBD component of the co-simulation was validated. A generic coupling was created and tested, and in addition a framework for development, verification and application of the co-simulation was developed [37]. Furthermore, a guideline has been developed for achieving stable and efficient co-simulations. This has shown to be a valuable tool for industrial design in general as well as for research of grab performance.

To achieve a calibrated co-simulation model for specific material, in this case iron ore pellets, a DEM material model of iron ore pellets was calibrated employing a set of laboratory experiments. This step is necessary to model the material behavior that also includes material-equipment interaction. In this paper, normal and tangential contacts are modelled using Hertz Mindlin (no-slip) model. Two settings have been used in the calibrated model; the Hertz-Mindlin model with angular movements restricted and the Hertz- Mindlin model with rotation enabled. The rotation-restricted model has been selected because Bierwisch Bierwisch, 2009 suggests that this can be useful when spherical particles are used. Restricting the rotation of particles has been used successfully to resemble realistic material behavior Mohajeri et al., 2020b, 2020a, 2021; [39]. The rotation-enabled model follows the recommendation by Ai et al. [40] to use model C for quasi-static simulations. Following the suggestion of Wensrich and Katterfeld [41], the rolling stiffness of Iwashita and Oda [42] is used and the viscous rolling damping torque is disabled.

Fig. 3 illustrates the calibration strategy for DEM input variables. Input variables are grouped into 3 divisions: A) particle property, B) particle-geometry interaction, and C) particle–particle interaction. In division A, the bulk density is calibrated by selecting a proper value for particle density (i.e. 3700 kg/m^3). In division B, a wall friction test is conducted and simulated by placing a single particle on horizontal plane tilting with an angular velocity of 30 degrees/s. To calibrate the particle-geometry static friction, the rotation of particles is restricted (in both experiment and simulation). Next, a proper value for particle-geometry rolling friction is selected, which is the only DEM parameter with a significant influence on rolling resistance. In division C, angle of repose tests as well as the penetration test with several tool shapes are calibrated by adjusting particle–particle static and rolling friction coefficients. In order to explore possible combinations between DEM input variables of division C, a full factorial experimental plan is used.

Together with the verified DEM-MBD co-simulation framework, the calibrated material model allowed to create a full-scale model of a scissors grab. To achieve reasonable computational times, several techniques were applied including stiffness reduction [43] and coarse graining [44].

- **Step 2. Validated scissors grab model**

The second step in the design framework focusses on validation of full-scale model of an existing grab in real operational conditions. In an earlier stage of this research an existing grab for iron ore was used as reference for the modelling. The large-scale co-simulation was validated using an existing cable operated grab in the reference case study. Cable operated grabs are the most common type in the bulk handling industry for the closing mechanism of grab. Fig. 3 (left) displays a four rope scissors grab that was used for our reference case. The four cable scissors grab consists of three parts: a left and right scissors half and a suspension part. Two hoisting cables are connected to the suspension part, which is connected to the two shells with chains. The full-scale scissors grab model was validated before the start of the actual design of a new grab. This was achieved by on-site experiments using full scale operational scissors grab with a bulk handling crane in the Netherlands. Several operational parameters were varied during the experiments while the payload, the torques and angular velocities of the winches were monitored and recorded. The grab's kinematics was captured by video tracking. The validation is shown in Section 3, including the experimental setup and the comparison between the measured and simulated properties.

- **Step 3. DEM supported design process**

This is the main step in the design framework as it relies on extensive DEM simulation. In this step the validated model of an existing operational grab is used to derive systematically new

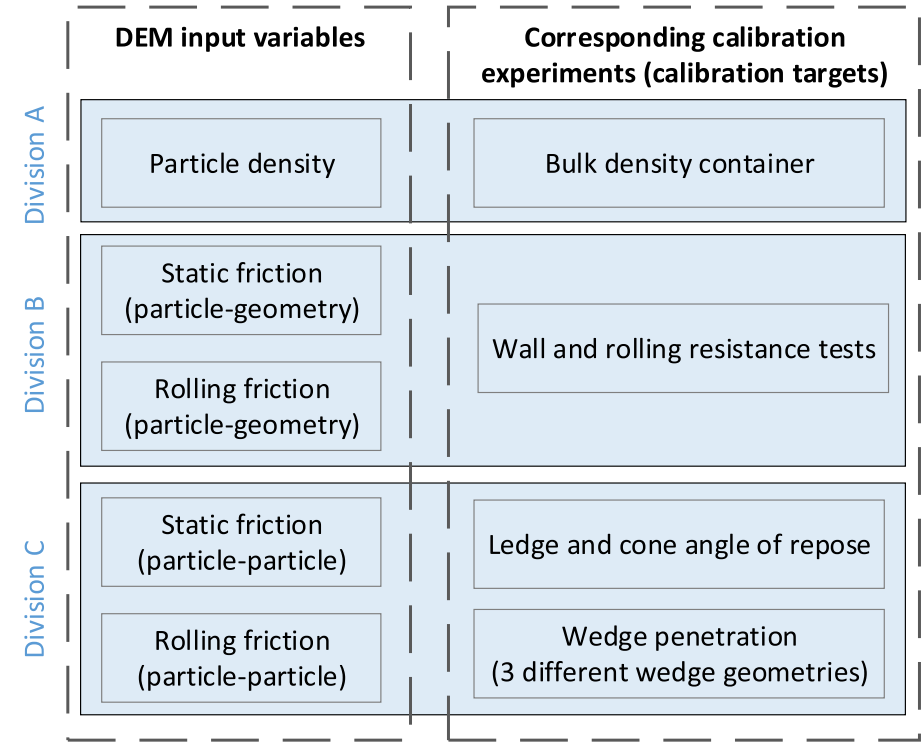

Fig. 3. DEM calibration strategy for a co-simulation of grab and iron ore pellets.

generation of grabs. Based on the validated model in the previous step, the effect of several design parameters on the grab's performance were investigated. To assess the grab performance several key performance indicators (KPIs) can be defined, including payload, digging path, spillage and closing resistance. For further details the reader is referred to the PhD thesis of Lommen [45]. The detailed insight in the grab's performance was then used in the design stage to develop a new generation of grabs. New shape geometries, closing mechanisms as well as different sizes of a new grab generation are derived in this step.

The new grab designs can be further analyzed and assessed with different KPIs by predicting their performance with the DEM-MBD co-simulation. Although the model used in the DEM-MBD co-simulation is validated with full-scale on-site tests for an already existing grab, the question remains whether the predicted performance of a new grab design will meet the behavior in reality. To answer this question, it is crucial to build a prototype and test it in real life operation conditions to confirm the predictions from the DEM-MBD co-simulation. This framework showed that the predicted performance matched the operational performance of the new grab, encouraging engineers to use this DEM supported design process for generating new shapes and sizes of grabs.

- **Step 4. Engineering and building a full-scale prototype**

Based on the new generated grab designs in step 3, a prototype can be further engineered and manufactured. The development of the nemaX®, a new generation of grabs, was the result of an iterative design process with in-house engineering and simulation supported design of step 3. Fig. 4 shows the scissors and nemaX grab together. For the nemaX both a new mechanism and a new shell shape were designed. The cable and sheave arrangements as part of the new mechanism allow faster opening and closing of the grab. Together with the new curved shape of the shell and the chain connecting points on the shell, the ratio between the forces exerted and the filling of the grab is optimized. Next to the lighter main hinge point and less sheaves, weight reduction of the grab was also achieved by lighter construction based on accurate insights into forces from our numerical approach. In brief, this new grab type compares to existing grabs by having a 30% larger footprint, reduced weight of 15% and increased opening and closing speed of 20%. This will result in a higher payload and lower cycle time, which is the overall goal in bulk material handling. The prototype was later used for the final step in the design framework to show that the predicted performance in the DEM-MBD co-simulation matches the operational performance of the grab with different bulk material under different operational circumstances.

- **Step 5. Prototype evaluation**

A new series of on-site experiments were designed and executed to test the nemaX® under different operational conditions such as on a prepared heap of iron ore pellets with a horizontal and inclined surface as well as in the ship. Also, the grab was tested on a variety of bulk materials, but for the focus of this paper here only the results of iron ore pellets are presented. Again, several operational parameters were varied while the payload and the torques on and angular velocities of the winches were closely monitoredand recorded during the grabbing process. The grab's kinematics was captured by video tracking. The results of these experiments are presented in Section 4.

- **Step 6. True validation independent form grab design**

To predict the performance of the new generation of grabs, nemaX®, a new virtual grab model was created for DEM-MBD co-simulation. The new virtual model was needed because the relevant grab characteristics were different from the scissors grab on which the model was initially validated in step 2. Moreover, the input for the closing and hoisting winches operated by the crane driver was updated to the values obtained from the on-site experiments. The comparison between the predicted performance and the grab's performance in the field tests was compared, and these results are shown in Section 5. This last step is called a true validation as the new grab design that came out from the grab independent design framework was prototyped and the behaviour of the DEM-MBD co-simulation matched the behaviour observed in practice of the full-size prototype of the new grab. True validation is completely independent from the co-simulation framework including material model and interaction properties.

3. Validated scissors grab model (Step 2 in design framework)

Based on the design framework, the validation of a full-scale model of an existing grab in real operational conditions is done in step 2. A full-scale scissors grab is validated to enable the start of new generation grab design. A series of on-site experiments were executed using full scale operational scissors grab with a bulk handling crane. While some operational parameters were varied, the payload, the torques on and angular velocities of the winches were constantly monitored.

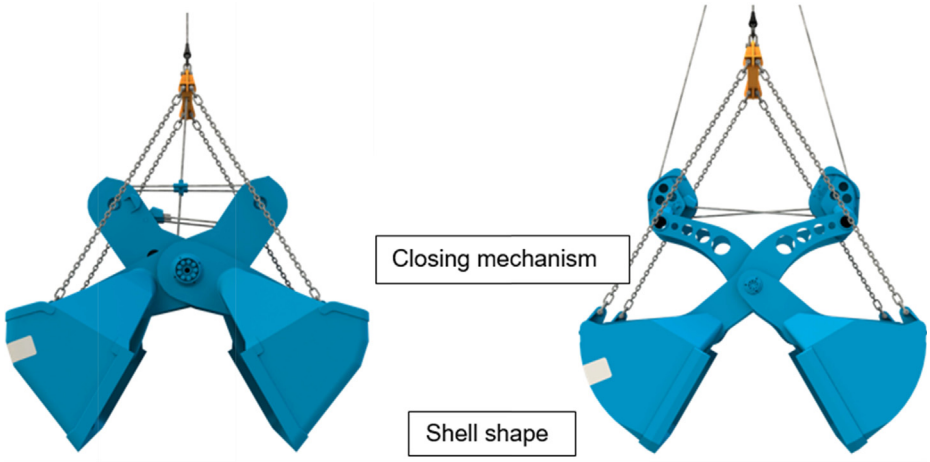

Fig. 4. Left: Scissors grab, and right: nemaX® (images: courtesy of NEMAG BV).

3.1. Virtual model

The virtual model for the scissors grab contains two coupled bodies (the two shells) that interact with the bulk material [36]. The ropes, chains, sheaves and suspension are not modelled in the DEM software and are only present in the multibody dynamics model because they do not interact with the particles. The shells are imported into EDEM® where their surfaces are meshed. The co-simulation setup is shown in Fig. 5. All the interaction forces between the surface elements and the particles are transformed into a force vector and a moment vector acting around the centre of mass of the bucket. These forces and moments are then communicated to the multibody dynamics model in Adams where they act on markers located in the centre of mass of coupled bodies. Particles are generated two seconds before the grab is expected to be in contact with the bulk material. The two seconds allow for the particles to settle completely while unnecessary computational costs are avoided. Another reduction in costs is achieved by simulating the first 15 s only in the MBD solver as there are no particles to be simulated yet, which means that there is no input from DEM for the MBD solver. This reduces the computational time with a factor of 100, as the overhead from the coupling is no longer required and the MBD solver can use much larger time-steps without compromising the stability of the results. To validate this model it is necessary to compare it with real operational data on site in a bulk terminal.

3.2. Experimental setup

To capture the grab's kinematics, a system for video tracking was installed (Fig. 6). The position and velocity of the grab were measured by analysing video captures of the closing process. The grab has been marked at three different locations, shown in Fig. 6. Two markers were placed on the buckets and a large marker was placed on the main hinge of the grab. Video was captured in Full HD resolution at 25 frames per second. This proved to be sufficient for tracking the motions of the three markers. The origin was set to the main hinge point marker when the grab was resting at the surface of the bulk material as shown by the axes in Fig. 6. For the tracking of the markers, the automatic tracking software Tracker (Brown) was used. Grab movements were captured in 2D because a side view for a second camera could not be obtained at

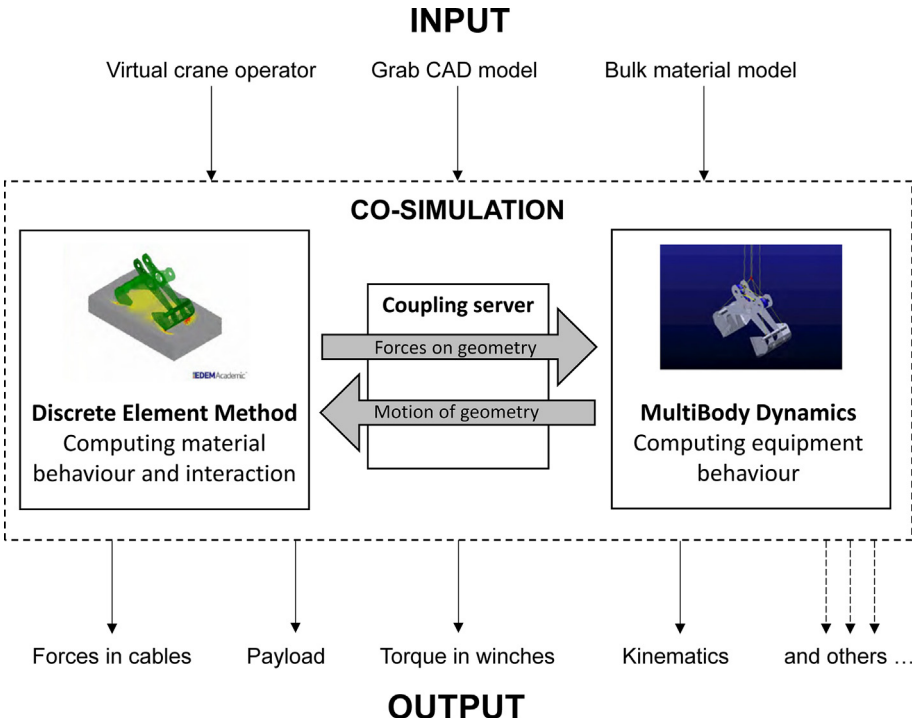

Fig. 5. Co-simulation setup. A coupling server exchanges information (forces on geometry and motion of geometry) from the DEM model (left) and the MBD model (right).

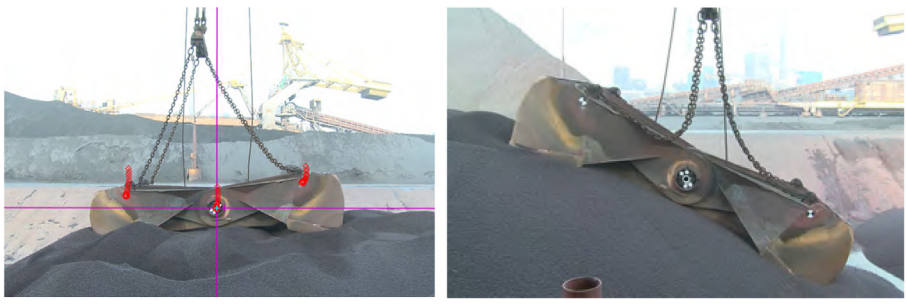

(a) (b)

Fig. 6. Experimental setup: origin and tracking of markers during the experiments a) Grab on flat surface b) Grab on sloped surface of 28 degrees.

the terminal. Measuring the position of the grab with accelerometers and a data-acquisition system mounted on the grab was considered unfeasible.

3.3. Validation results

This section compares the prediction of the configured co-simulation with the tests conducted on the terminal. The grab performance was analysed in 2 scenarios of bulk surface materials: flat and sloped (Fig. 6). First the flat surface is examined, followed by the sloped surface. After validating the coupled model on flat surfaces, a sloped surface is simulated to investigate whether the validation can be expanded. Fig. 5 shows a screenshot taken from the flat surface (Fig. 6a)) and sloped experiment (Fig. 6b)), showing that the grab has penetrated the pile of iron ore pellets at an angle of 28 degrees.

The flat surface experiment has been conducted three times, and the results show mass of iron ore pellets displayed in Table 1, averaging to a 27.8 tons per cycle. These experiments have each been simulated with the no-rolling material model, resulting in an average load of 27.5 tons. The small differences in outcome can be explained through the variation in the bulk material surface, operating characteristics and numerical scatter. Compared to the measurements on the flat surface, which grabbed an average of 27.8 tons, the sloped surface measurement grabbed less at 26.4 tons. The co-simulation predicted a load of 25.7 tons and was able to predict the loading of the grab on the sloped surface just as well as on the flat surface.

The comparison of the measured load on the crane in simulation and experiment is shown in Fig. 7. The tensile forces in the four cables operating the grab are measured using load cells. The load cells are located adjacent to the driving winches of the crane. These load cells as well as other sensors are calibrated by the terminal operator on a regular basis. The load cells measure force in cables with a frequency of 2 Hz. The desired coefficient of determination [46], to show the experimental validation, is R^2 >= 0.9 for force on cables and R^2 >= 0.8 for the torque in winches. The chosen R^2 values mean that respectively 10% and 20% of the variance can be attributed to unknown variables such as modelling errors, measurement errors and variability caused by the manual operation and swinging of the grab, irregularities in the bulk material surface and other external factors. The modelled winches do not have a brake and have to hold the drum in position by exerting a torque, which explains the difference in the opening stage. Also likely caused by the absence of a load balancer in the model. However, considering the fact that the hoisting cables will be tensionless during the grabbing of the bulk material, this variance is not conceived as too high for a co-simulation of a closing grab. Furthermore, the chose values for R^2 take into account unknowns and losses in the driveline of the crane used for the experiments.

For the flat surface the co-simulation predicts the increasing load during closing (C) due to the grabbing of material quite well, with a coefficient of determination 0.928, which exceeds the required 0.9. During hoisting (H) a peak is visible in experimental signal at approximately t = 26 s which is not shown by the co-simulation, likely caused by a slight difference in cable slack between model and experiment. During suspension (S) it can be noted that the co-simulation damps out quicker than the experiment. This is because the simulation takes a rope of 20 m into account, compared to a rope length of more than 100 m in reality. Apart from these differences, this comparison demonstrates that the whole loading process of the grab can be accurately predicted. For the sloped surface the comparison of the measured load on the crane in simulation and experiment show even better results (Fig. 7b), due to the absence of fluctuations on the sloped surface in the experiment. The sloped surface signals correlate with a R2 = 0.958, well above the desired 0.8 and therefore the load validation can be expanded to sloped surfaces.

The winches of the crane control the motion of the grab and in order to maintain the assigned winch velocities, torque is required. Fig. 8 shows the torque of the closing and hoisting winch during a grab cycle. When the grab opens and lowers (L), agreement is off

Table 1
Grabbed material in experiments and simulation.

		Exp. No	Experiment mass (ton)	Simulation mass (ton)
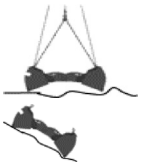	Experiment 1	1.1	27.2	28.1
	Flat surface	1.2	27.9	27.8
		1.3	28.3	26.6
		Average	**27.8**	**27.5**
	Experiment 2	**2.1**	**26.4**	**25.7**
	Sloped surface			

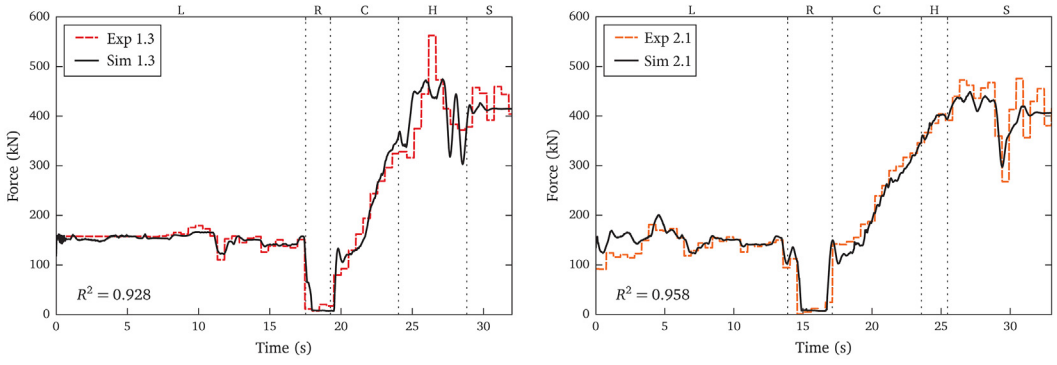

a) flat surface b) sloped surface

Fig. 7. Load comparison between a) simulation 1.3 and experiment 1.3 with a flat surface; b) simulation and experiment with a sloped surface: simulation 2.1 and experiment 2.1. Grab operation consists of lowering of the grab (L), resting on the surface (R), closing (C), hoisting (H) and being suspended from the crane (S).

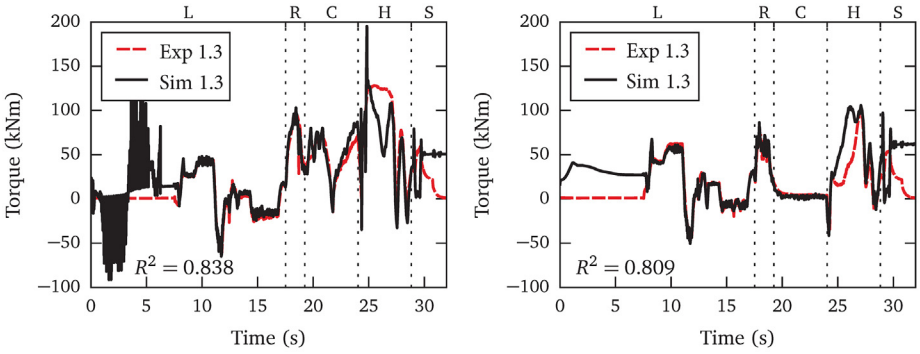

(a) Closing winch torque.

(b) Hoisting winch torque.

Fig. 8. Closing and hoisting torque during simulation 1.3 and experiment 1.3 with a flat surface. Grab operation consists of lowering of the grab (L), resting on the surface (R), closing (C), hoisting (H) and being suspended from the crane (S).

during the first nine seconds. In the experiment, the grab starts opened while in the simulation the grab starts closed, resulting in additional closing torques to open the grab. For the hoisting winch, the brake is activated during the suspension period (S) in the experiment while the simulation lacks a winch brake. The predicted closing winch torques have a correlation coefficient of 0.838 in the closing stage (C), approximating the experiment sufficiently. In the hoisting stage a deviation can be noticed, which is caused by a slightly shifted equilibrium between closing and hoisting cables. However, when both the closing and winch torques are combined a hoisting correlation of 0.809 is achieved. These results confirm that the forces required for closing and hoisting a grab with iron ore pellets are correctly predicted.

Fig. 9 shows the position of the markers in the simulation and experiment. The vertical movement of the virtual main hinge point can easily be matched to the position of the markers during the experiment. The vertical movement of the buckets shows also similar good vertical match with correlation coefficients exceeding 0.975, well above the desired $R^2 > 0.9$. The small horizontal movement of the main hinge point in the experiment is very likely the result of a slightly asymmetric surface, which was not present in the co-simulation. This horizontal displacement is also visible in the horizontal position of the left and right markers, both shifted to the left. Overall, the dynamics of the grab during closing are predicted very well, except for the horizontal shift likely caused by the irregular bulk surface.

The confidence interval of the simulation determines how many times a simulation needs to be repeated for achieving a reliable mean value. For the grab simulation, a 95% confidence interval is considered adequate and a maximum interval size of 5% is used. The simulation of experiment 1.3 is performed three times to see whether these conditions can be met. The comparison of the measurements taken in experiment 1.3 and simulation 1.3 are shown in this paper, for the other cases is referred to [45]. The observed comparisons shown in Fig. 8 validate that the developed coupled models can predict grab performance. Overall, the validation presents a virtual grab model interacting with virtual iron ore pellets, with behavior similar to their physical counterparts. This validation leads to the outcome of step 2 in the design framework validated models of existing grabs, clearing the way for the design of new generations of grabs.

4. Design parameter sensitivity analysis and virtual prototyping (Step 3: DEM supported design process)

The grab performance in real working environment can be observed in different ways, for example by examining the mass of the material in the bucket, the stress network of the compressed particles or the relative sliding wear. These analyses can be challenging to extract in real working conditions, however the simulations of the process can provide the designer with such data. Even though simulations are very rich in results, analysing and comparing prototypes becomes an intensive task based on the variations of parameters in each simulation setup. While running experiments the grab performance can be quantified by examining the load, torque and motion of the grab during closing. These data were convenient to measure with the use of the sensors present in the crane and an analysis of captured video recordings that offered a satisfactory basis for validation the behaviour of the virtual grab. However, a wider range of data is available or can be extracted from the co-simulation. When evaluating prototypes, additional data of the simulation can therefore be used in quantifying and understanding the performance of a virtual prototype. The next step is to systematically define key performance indicators to provide designers quick and reasonable quantified analyses. This brings understanding and sensitivity analyses, otherwise impossible to obtain.

4.1. Key performance indicators (KPIs)

To capture the performance of a virtual grab prototype quickly, six Key Performance Indicators (KPIs) were defined and quantified. Here, in this paper, we present only 2 KPIs, while the others are detailed in the PhD thesis of Lommen [45]. These KPIs are the core of Step 3 in the Design framework as they allow for systematic quantitative comparison between prototypes, giving designers the possibility to detect trends and select the best prototype for a selected number of scenarios. The KPIs focus solely on different aspects of the performance of a prototype. Operating costs, production or other engineering aspects such as strength, stiffness or fatigue are not taken into account at this stage. The six KPIs are defined in the Table 2. The definition of the KPIs came from years of experience in grab performance analyses, and the process took multiple iterations to ensure robustness of the KPIs for different grab designs and scenarios. All six KPIs have been mathematically defined in order to provide measurable design parameters to engineers.

Grab unloading systems are usually evaluated by comparing the hoisted mass to the hoisting capacity of the grab crane. Obviously, the combined mass of grab and material needs to be below the hoisting capacity of the crane, however the performance of a grab focusses on the ratio between the grab weight and grabbed bulk material. Ideally, the entire hoisting capacity is used for hoisting bulk material during each cycle, however, a grab needs its mass

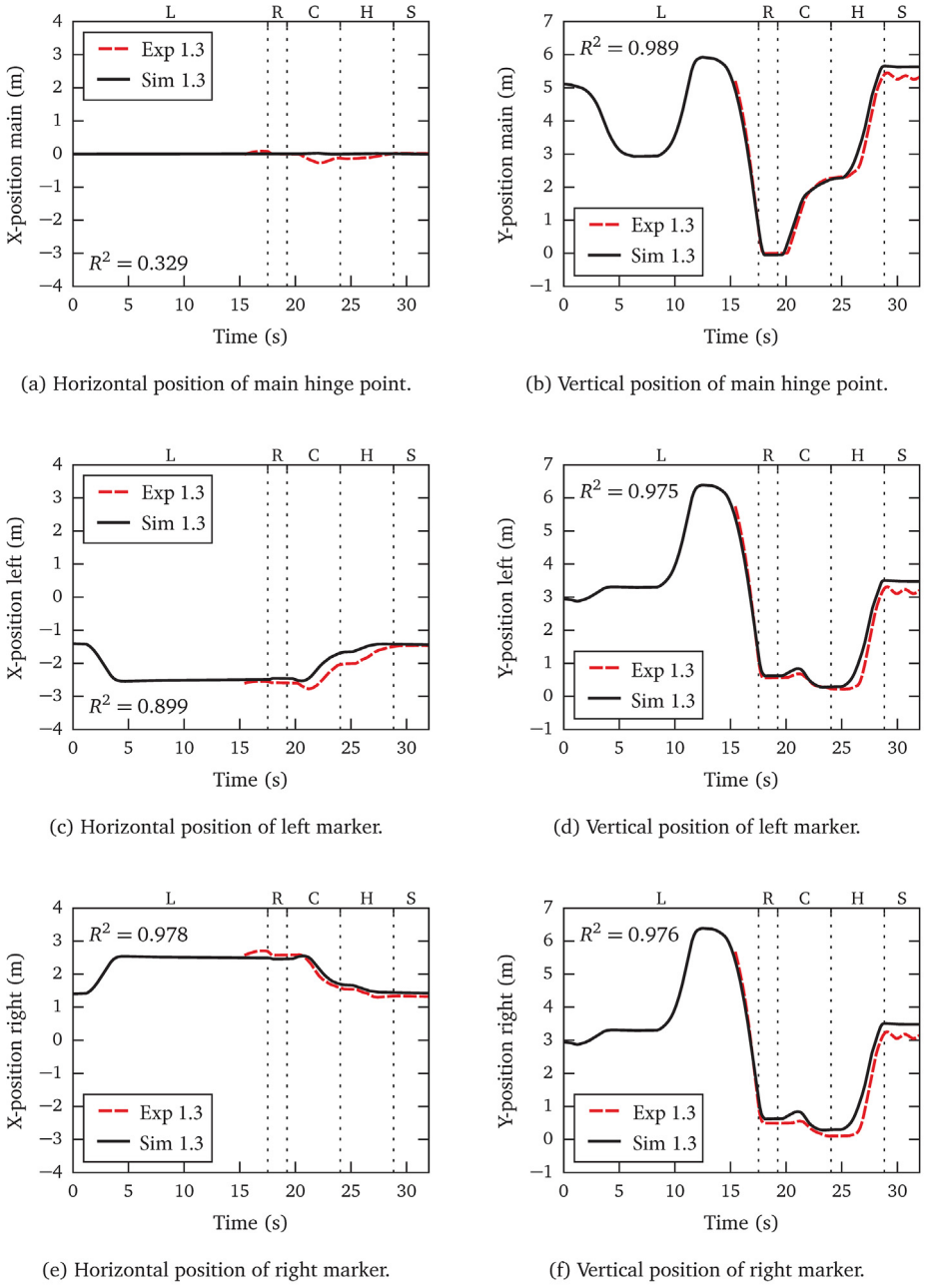

(a) Horizontal position of main hinge point.

(b) Vertical position of main hinge point.

(c) Horizontal position of left marker.

(d) Vertical position of left marker.

(e) Horizontal position of right marker.

(f) Vertical position of right marker.

Fig. 9. Comparison between simulating and video-tracking of the three applied markers on the grab, on flat surface experiment 1.3. Grab operation consists of lowering of the grab (L), resting on the surface (R), closing (C), hoisting (H) and being suspended from the crane (S).

for penetrating the material, as well as its structural strength and being able to maintain a long lifespan.

The mass indicator ψ_{mass} compares the amount of grabbed material to the weight of the grab by means of Equation (1):

$$\psi_{mass} = \frac{m_{DWT} + m_{spillage}}{m_{grab}} \tag{1}$$

where m_{grab} is the mass of the grab, m_{DWT} is the mass of the bulk material inside the grab and $m_{spillage}$ is the mass of the bulk material spilled over the sides of the grab after closing. Spilled material is taken into account to focus on the effectiveness of the grabbing process, without possible influences of a limiting bucket capacity. As a result, the prototypes are evaluated on their grabbing performance and not whether the bucket is sufficiently large.

The grab efficiency indicator $\psi_{grabefficiency}$ indicates the efficiency of the closing. During closing the grab moves through the bulk material, displacing the particles that are inside the closing trajectory. Ideally, all the material inside the closing trajectory ends up being picked up by the grab and no effort is wasted on material that leaks between the two knives during closing. The grab efficiency is defined according to Equation (2) as the ratio between the bulk material that has been grabbed (the material inside m_{DWT} and the mass spilled over the sides $m_{spillage}$) and the bulk material inside the closing path $m_{closingpath}$.

$$\psi_{grab\ \ efficiency} = \frac{m_{DWT} + m_{spillage}}{m_{closingpath}} \tag{2}$$

The bulk material $m_{closingpath}$ is calculated by computing the enclosed area based on the closing trajectory and multiplying by

Table 2
KPIs for grab design.

KPI name	Description
Mass indicator ψ_{mass}	The ratio between the bulk material mass captured by the buckets and the weight of the buckets.
Grab efficiency indicator$\psi_{grabefficiency}$	The ratio between the grabbed bulk material (material inside the buckets and the mass spilled over) and the material inside the closing path.
Volume indicatorψ_{volume}	The comparison between the volume of the grabbed material to the overall defined volume of the grab.
Spillage indicator$\psi_{spillage}$	The level of spillage of the grab which happens if the bucket volume of the grab is smaller than its digging capacity.
Closing resistance indicator$\psi_{closingresitance}$	The energy required for closing the grab while grabbing material.
Closing time indicator$\psi_{closingtime}$	The time it takes to complete the grabbing of the material.

the width of the grab (w) and the bulk density. The bulk density of the untouched bulk material is measured before penetration occurs by counting the mass of the particles present in a defined volume underneath the surface of the bulk material. The rest of the KPIs are defined in a similar way and enable quick comparison of designs in parametric variations of geometry.

4.2. Parametric variations

By studying the variation of a single grab parameter, its effect on grabbed mass, efficiency and spillage become visible. This confirms the value of the KPIs for evaluating grab performance, and improve the understanding of the relations between grab parameters and grab performance. The performance of a grab unloader depends on many design variables and customer preferences. Grab unloader operators select a suitable grab based on their preferences on unit price, operating costs and unloading capacity.

In this work we select four parameters of a scissors grab (the grab mass and 3 dimensions of the buckets) to perform a parametric study and present the grab behavior. The parameters are labeled as the mass of a grab *m*, the width of a grab *w*, the length of a grab *l*, and the height of a grab *h*. The parameters are displayed in Fig. 10 and there are 5 variations of each parameter equally distributed between 80% and 120% of the original value of the analyzed scissors grab. In the first set displayed, the mass is varied while the *w, l* and *h* dimensions are kept constant and thus the volume of the bucket remains constant as well. In the three other sets, the volume is affected by the change in either *w, l* and *h*, while the mass of the prototype is constant. Changes in KPIs are considered significant when the new KPI lies outside the confidence intervals defined in Section 2 Step 2. By isolating these parameters one by one, their influence on the KPI becomes clear, allowing for a smart selection of virtual prototypes to be tested.

To operate the virtual prototypes in the co-simulation, a virtual grab operator has been introduced based on the measured operator characteristics on a real bulk terminal. The virtual operator opens the grab, lowers the grab towards the bulk material surface with a rate of 1.6 m/s until contact has been made and the grab penetrates the bulk material. Closing winch direction is then reversed, resulting in the closing in the grab. In practice, the hoisting winch aids in hoisting the grab due to the limited strength of the closing winch and cables. This does not require consideration in the virtual environment, where the hoisting of the grab can be achieved completely by the closing winch and cables. The grab mass affects the strength and stiffness of a grab and determines the mass ratio. The closing path of grabs with a different mass is shown in Fig. 11, where it can be observed that the changes in mass mostly affect the initial penetration. Heavier grabs penetrate deeper than lighter grabs and this results in a larger volume of material touched.

The effects of changes in mass and penetration causes on the first two KPIs (Mass indicator ψ_{mass} and Grab efficiency indicator $\psi_{grabefficiency}$) can be seen in Fig. 12. The mass indicator in Fig. 12a) shows that the heavier grabs negatively impact the mass ratio, favouring lighter grabs, although the mass is also required for the strength and stiffness of the bucket. The grab efficiency indicator in Fig. 12b) reveals that the additional material in the deeper closing paths of heavier grabs also results in a lower grab efficiency. The heavy grabs loose part of the additional material during the

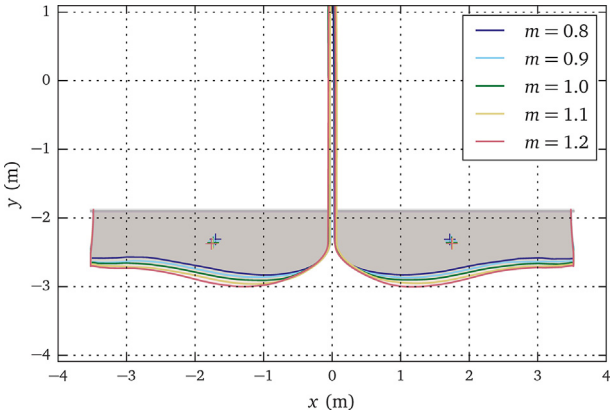

Fig. 11. Closing trajectory for grabs with varying mass.

m	0.8	0.9	1.0	1.1	1.2

(a) Mass.

w	0.8	0.9	1.0	1.1	1.2

(b) Width.

l	0.8	0.9	1.0	1.1	1.2

(c) Length.

h	0.8	0.9	1.0	1.1	1.2

(d) Height.

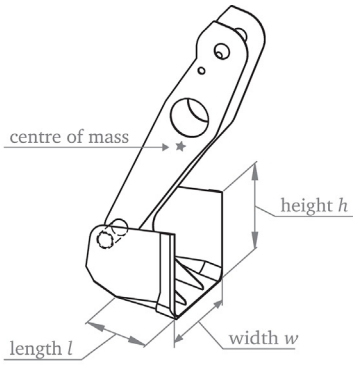

Fig. 10. Grab parameters with w, length l and height h. The mass m is equally distributed around the centre of mass.

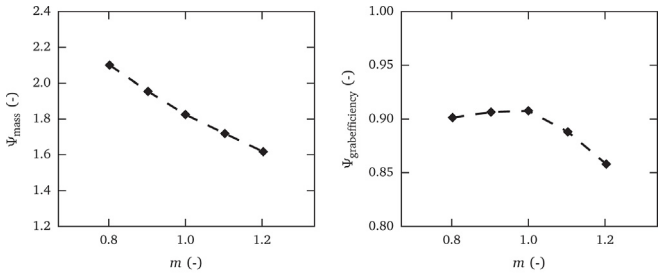

(a) Mass indicator. (b) Grab efficiency indicator.

Fig. 12. Effects of grab by parameter variation of the mass m. The grab with the original mass m_{grab} has m = 1.

closing of the buckets, with large amounts of material leaking between the two knives. In summary, the heavy grabs are less efficient when it comes to transferring the material inside the closing path to the inside of their buckets. The capacity of these grab prototypes remains unaffected because the dimensions of the grab (l, w, h) are kept constant. As the amount of material grabbed becomes less for the lighter grabs, the volume indicator reduces. This indicates that the grab is not filled completely.

Studying the effects of grab parameters contributes significantly to the understanding of the grab performance overall. The single parametric variations are quite limited examples of virtual grab prototyping, as in developing a new prototype there is no need to restrict to a single variable, also combinations can be

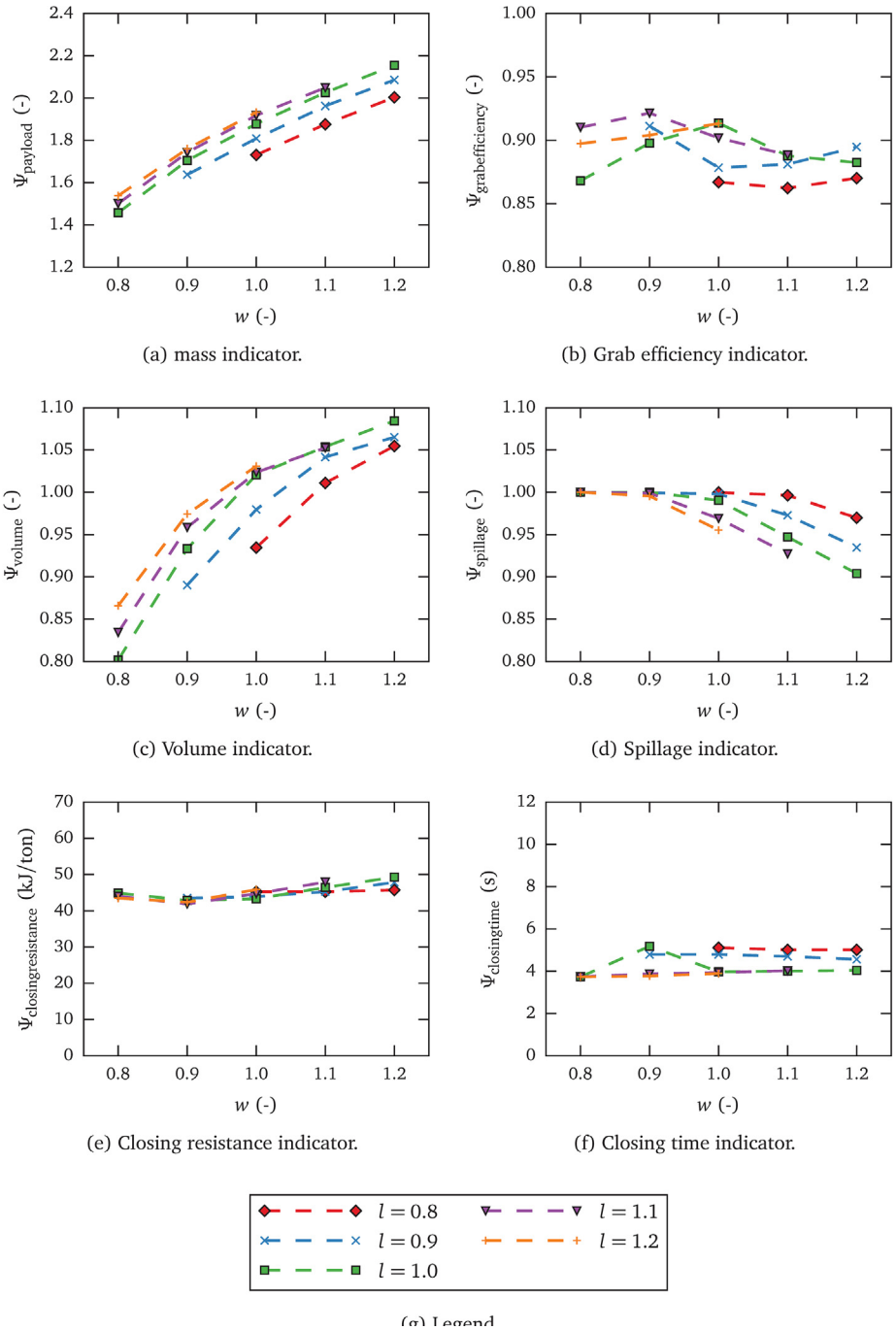

(a) mass indicator. (b) Grab efficiency indicator.

(c) Volume indicator. (d) Spillage indicator.

(e) Closing resistance indicator. (f) Closing time indicator.

(g) Legend

Fig. 13. The performance of the virtual grab prototypes.

investigated. The understanding is the initial step before going into optimal combinations of design parameters for maximum grab performance.

4.3. Virtual prototyping

The parametric variation led to the design of 18 new virtual prototypes, each having a different combination of length, width and height dimension. These prototypes have an equal bucket volume indicated in Fig. 13, identical to the KPI volume of the reference grab. Table 3 shows the dimensions of 18 grab prototypes and one reference grab (l = 1, w = 1 and h = 1). The maximum variation of the dimensions is set at 20% compared to the reference grab to keep changes compatible to the strength and stiffness of the prototypes. Mass of the prototypes is calculated by adding the difference in bucket material mass to the reference grab, as shown in Table 4. The colours used in the Tables 3 and 4 are related to the results in Fig. 13.

The performance of the prototypes has been summarized in Fig. 13, supporting several observations and conclusions drawn for the grabs' performance. In general the mass performance of the prototypes with a large length exceeds those with less length (Fig. 13a). Likewise, prototypes with a larger width exceed those with less width. Although all prototypes share the same bucket volume, a look at Fig. 13c and 13d tells that several prototypes cannot fill this volume, underperforming compared to the reference grab. With a relatively wide grab, making the buckets longer results in a higher grabbing efficiency (Fig. 13b), as there is more space available in the length direction to accommodate particles entering the bucket. According to Fig. 13f, large changes in closing time are not predicted as expected, as all prototypes use the same type and dimensions of the closing mechanism. The closing resistance indicator slightly favors wider grabs, as the side knives of these grabs experience less resistance. The grab efficiency indicator shows that some prototypes have a higher efficiency in moving touched material into their buckets, influenced by the combined effects of changing length, width, height and mass.

The prototypes with $\psi_{volume} > 1.014$ show a clear improvement in grabbed material as the grabbed material exceeds the bucket volume identical to that of the reference grab. For example, the grab with l = 1.0 and w = 1.2 has $\psi_{volume} = 1.084$, which means it has 6.9% more material in its buckets. In addition, spillage of this prototype changes from $\psi_{spillage} = 0.991$ to $\psi_{spillage} = 0.904$, spilling 8.8% more material compared to the reference grab, indicating that more material has been grabbed than it could be handled by the buckets. This leads to the new prototype grabbing 2.155 times its own mass instead of $\psi_{mass} = 1.874$, an impressive increase in grabbed material of 15.0% (Fig. 12a). As a result, the payload of the grab unloader system improves from 1.868 to 1.948, an increase of 4.2%, strongly limited by the size of the buckets. When the bucket size is matched to the grabbing performance and thus spillage is prevented, a prototype with an attractive payload ratio increase of 15.0% should be possible. Although these prototypes are not immediately ready for production and might require additional engineering, these results demonstrate that virtual prototyping can lead to significant potential improvements of grab designs.

This demonstration showed that grab performance can be evaluated in 3 distinct ways:

1. Prototypes can be compared fast and clearly with the help of six KPIs, where changes in mass, grabbing efficiency and spillage are easily detected.
2. More insight into the interaction between prototype and material is achieved in a graphical comparison of closing trajectories of the prototypes.
3. A prototype can also be analysed in detail, for example by studying stress concentrations on the buckets, aiding in preventing heavy localised wear on the buckets.

With the help of these grab analysis tools, virtual prototypes of grabs can be analysed thoroughly and swiftly. When virtual prototyping is implemented in the design process of grabs, significant gains are achieved. According to the preferences of grab customers, engineers can develop prototypes and test these in the virtual environment, establishing a fast and affordable alternative to the building and testing of physical prototypes.

5. Extended validation: Comparison predictions and experimental results grab prototype (Step 6. True validation independent form grab design)

A new prototype was engineered and built using the results of the previous step. The experimental results of the newly built grab prototype (shown in Fig. 3) are compared with predications of the co-simulation. Three experiments on flat surfaces are selected to validate the co-simulation for the grab prototype. As shown in Table 5, the experiments and simulations compared well in terms of the average mass of 34.2 and 34.3 tons of iron ore pellets per cycle, respectively. The margin of error for the experiments is 1.2 and for the simulation is 2.8 tons mass. This small difference is probably caused by the variation in the bulk material surface, operating characteristics and numerical scatter.

To further validate the co-simulation from various aspects, experiment 3.3 and simulation 3.3 are selected for detailed analysis. Fig. 14 compares the total force on the cables between the experiment and simulation. Apparently, the grab touches the material slightly earlier in the simulation, which caused the small

Table 3
Height of the virtual prototypes.

l \ w	0.8	0.9	1.0	1.1	1.2
0.8	-	-	1.16	1.056	0.98
0.9	-	1.18	1.07	0.98	0.91
1.0	1.23	1.10	1.00	0.91	0.84
1.1	1.16	1.04	0.94	0.86	-
1.2	1.10	0.98	0.88	-	-

Table 4
Mass of the virtual prototypes.

l \ w	0.8	0.9	1.0	1.1	1.2
0.8	-	-	0.986	0.987	0.989
0.9	-	0.995	0.993	0.993	0.995
1.0	1.008	1.002	1.000	1.000	1.005
1.1	1.016	1.010	1.007	1.010	-
1.2	1.023	1.017	1.015	-	-

Table 5
Collected bulk material (payload) using the grab prototype in experiments and simulations.

Flat	Experiment mass (ton)	Simulation mass (ton)
3.1	32.8	31.5
3.2	34.0	35.4
3.3	36.0	36.0
Average	34.2	34.3

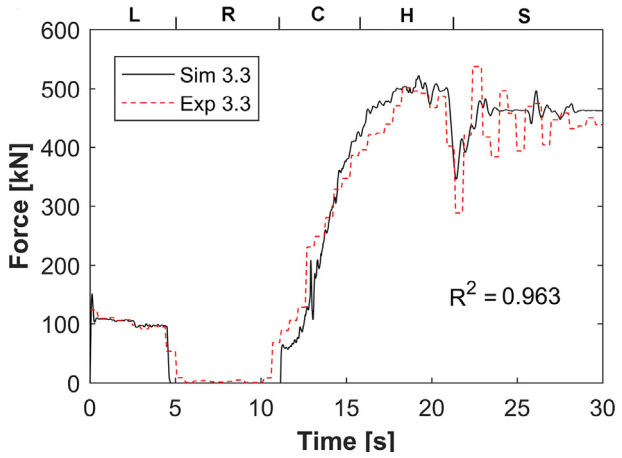

Fig. 14. Load comparison between experiment 3.3 and simulation 3.3; Grab operation consists of lowering of the grab (L), resting on the surface (R), closing (C), hoisting (H) and being suspended from the crane (S).

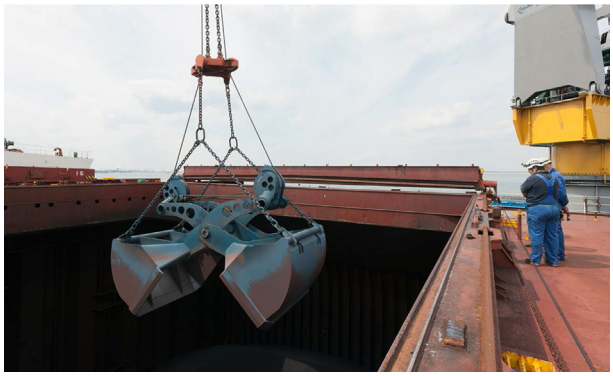

Fig. 16. Full size prototype of the new generation of grab designed with DEM support.

deviation during closing and hoisting stages. The force over all stages is predicted accurately with an overall correlation coefficient 0.963.

To validate the grab dynamics, the torque of the closing and hoisting winches during a grab cycle are compared in Fig. 15. Similar to the force data (Fig. 14), the torque in the closing and hoisting winches are predicted adequately. Only during the suspension stage, the torque starts to deviate from the experimental data, for both hoisting and closing winches. A brake is activated in the experiment after the hoisting to prevent overheating the electric drives resulting in a torque decrease, while the simulation lacks a winch brake and the torque remains constant. If we ignore the data after activating the brake, the predicted closing and hoisting winches have correlation coefficients of 0.964 and 0.936 respectively. These results confirm that the prototype's dynamics are correctly predicted in the simulation.

The on-site experiments in real operational bulk terminal with the new grab prototype (Fig. 16) compared well to the predictions of the validated DEM-MBD model. With this a true validation has been established and a model has been achieved that is independent of a specific grab design. With this the full design cycle (shown in Fig. 2) is closed.

This last step in the design framework Step 6: True validation of a full-size model of a new generation of a grab with a full-size prototype in real operational conditions, closes the design cycle. This proves that this approach can be used for novel grab designs that can lead to breakthrough innovations in the market of granular material handling equipment. This framework paves the way for utilizing DEM-MBD co-simulation and their detailed features for defining different KPIs for quick performance comparison. This can support designers in making educated decisions in the engineering process of grabs. It can also give more insight into the possibilities to the grab users in the optimal operation of the grab and maximizing performance. The goal is to exploit the grab in maximum capacity as long as possible, and the DEM analyses can provide guidance on how to operate the grab in optimal operational manner based on the state of the material that is being handled as well as the type of the crane responsible for operation. By predicted and controlled grab behavior, the maintenance of the grab can by drastically reduced.

6. Conclusion

This study presented a design framework for novel designs of granular material equipment. The framework was tested by developing an improved grab design and predicting its performance. Experiments with the original design and newly built prototype compared well to the predictions of the validated DEM-MBD model used in the framework. This true validation proves that a full design cycle can be accomplished completely independent from a specific grab design. The fully completed design cycle is a breakthrough in the grab development. The same design framework can be used and adjusted for other types of bulk materials handling equipment.

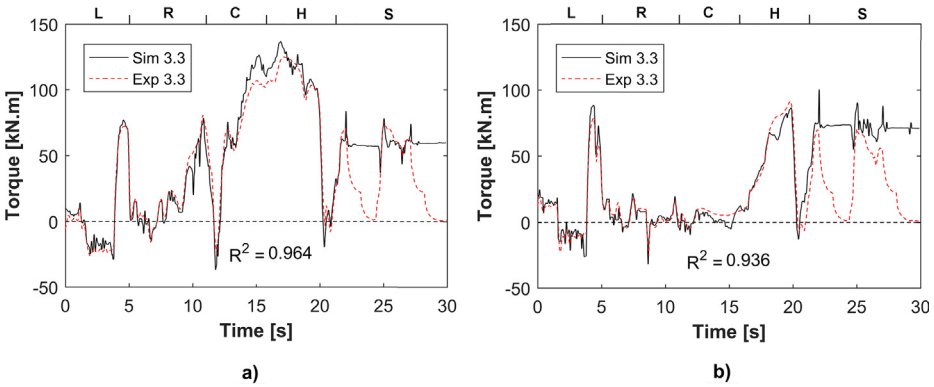

Fig. 15. Comparing torque in the winches. Left: closing winch; right: hosting winch; Grab operation consists of lowering of the grab (L), resting on the surface (R), closing (C), hoisting (H) and being suspended from the crane (S).

The 6 steps in the design framework are necessary to ensure reliability in the DEM supported design of new generation of grabs. With true validation the designers can fully trust the outcome of the simulation independent of the design parameters. Designers and engineers can use the results from the co-simulation to extract valuable information of the grab performance and understand closely the interdependence of the grab shape and closing mechanism with the materials state and operational conditions.

The developed and presented design framework in this work is beneficial to all parties concerned in the grab manufacturing industry. The design framework offers application-driven design of grabs where the customer's specific requests can lead to custom-made grab design by the manufacturer. The terminal operators can use this design framework in grab performance analysis and logistics planning. Environmental impact and energy consumption can be extracted from the design framework if necessary, supporting the stakeholders in the modernization towards impactless material handling systems.

This design framework is just the first step into new grab independent designs and can be adjusted to take into account variation of granular materials as well as variation in operational conditions. Future work includes adjustment of the design framework for different granular material handling equipment and developing models that capture materials' state in interaction with the equipment. Another valuable aspect is the environmental impact. Defining KPIs that take into consideration the impact of the granular material on the environment while being handled can bring us closer towards designing new generation grabs that minimize the environmental impact. This has the potential to revolutionize the bulk material handling supply chain for the benefit of all.

Funding

This work was supported by Nemag BV.

Declaration of Competing Interest

The authors declare that they have no known competing financial interests or personal relationships that could have appeared to influence the work reported in this paper.

Acknowledgments

The authors acknowledge Tata Steel (IJmuiden), and in particular Hans Schoorl, GSL (Grondstoffen Logistiek) andthe Raw Material Handling department for setting up the on-site experiments and the support in execution thereof.

References

Cundall, P.A., Strack, O.D.L.,]. A discrete numerical model for granular assemblies. Geotechnique 29 (1), 47–65.
Cleary, P.W.,]. Large scale industrial DEM modelling. Eng. Comput.
Cleary, P.W.,]. DEM prediction of industrial and geophysical particle flows. Particuology 8 (2), 106–118.
Balevičius, R., Kačianauskas, R., Mroz, Z., Sielamowicz, I.,]. Analysis and DEM simulation of granular material flow patterns in hopper models of different shapes. Adv. Powder Technol. 22 (2), 226–235.
Cheng, H., Shuku, T., Thoeni, K., Tempone, P., Luding, S., Magnanimo, V.,]. An iterative Bayesian filtering framework for fast and automated calibration of DEM models. Comput. Methods Appl. Mech. Eng. 350, 268–294.
Do, H.Q., Aragón, A.M., Schott, D.L.,]. A calibration framework for discrete element model parameters using genetic algorithms. Adv. Powder Technol. 29 (6), 1393–1403.
Pachón-Morales, J., Do, H., Colin, J., Puel, F., Perre, P., Schott, D.,]. DEM modelling for flow of cohesive lignocellulosic biomass powders: Model calibration using bulk tests. Adv. Powder Technol. 30 (4), 732–750.
Mohajeri, M.J., Huy, Do, Schott, D.L.,]. DEM calibration of cohesive material in the ring shear test by applying a genetic algorithm framewrok. Adv. Powder Technol., 112–125
Mohajeri, M.J., Helmons, R., van Rhee, C., Schott, D.L., 0]. A hybrid particle-geometric scaling approach for elasto-plastic adhesive DEM contact models. Powder Technol., 72–87
Coetzee, C.J., Horn, E., 1]. Calibration of the Discrete Element Method Using a Large Shear Box. Int. J. Mech. Aerosp. Ind. Mech. Manuf. Eng. 8 (12), 2105–2114.
Coetzee, C.J., 2]. Review: Calibration of the Discrete Element Method. Powder Technol. 310, 104–142.
Coetzee, C.J., Els, D.N.J., 3]. The numerical modelling of excavator bucket filling using DEM. J. Terramech. 46 (5), 217–227.
Coetzee, C.J., Nel, R.G., 4]. Calibration of discrete element properties and the modelling of packed rock beds. Powder Technol. 264, 332–342.
Coetzee, C.J., 5]. Calibration of the discrete element method and the effect of particle shape. Powder Technol. 297, 50–70.
Pachón-Morales, J. et al., 6]. Potential of DEM for investigation of non-consolidated flow of cohesive and elongated biomass particles. Adv. Powder Technol., 1500–1515
Wang, D., Servin, M., Mickelsson, K.-O., 7]. Outlet design optimization based on large-scale nonsmooth DEM simulation. Powder Technol. 253, 438–443.
Zhao, L., Zhao, Y., Bao, C., Hou, Q., Yu, A., 8]. Laboratory-scale validation of a DEM model of screening processes with circular vibration. Powder Technol. 303, 269–277.
Ucgul, M., Fielke, J.M., Saunders, C., 9]. Defining the effect of sweep tillage tool cutting edge geometry on tillage forces using 3D discrete element modelling. Inform Process. Agric. 2 (2), 130–141.
Ucgul, M., Fielke, J.M., Saunders, C., 0]. 3D DEM tillage simulation: Validation of a hysteretic spring (plastic) contact model for a sweep tool operating in a cohesionless soil. Soil Tillage Res. 144, 220–227.
Li, Y.-W. et al., 1]. Laboratory-scale validation of a DEM model of a toothed double-roll crusher and numerical studies. Powder Technol. 356, 60–72.
Yang, P., Zang, M., Zeng, H., Guo, X., 2]. The interactions between an off-road tire and granular terrain: GPU-based DEM-FEM simulation and experimental validation. Int. J. Mech. Sci. 105634
Bierwisch, C.S., 2009. Numerical simulations of granular flow and filling. Fraunhofer http://publica.fraunhofer.de/documents/N-438914.html.
Cai, R., Zhao, Y., 3]. An experimentally validated coarse-grain DEM study of monodisperse granular mixing. Powder Technol. 361, 99–111.
Kureck, H., Govender, N., Siegmann, E., Boehling, P., Radeke, C., Khinast, J.G., 4]. Industrial scale simulations of tablet coating using gpu based dem: A validation study. Chem. Eng. Sci. 202, 462–480.
Shen, J., Wheeler, C., Ilic, D., Chen, J., 5]. Application of open source FEM and DEM simulations for dynamic belt deflection modelling. Powder Technol. 357, 171–185.
Yinyan, S., Man, C., Xiaochan, W., Odhiambo, M.O., Weimin, D., 6]. Numerical simulation of spreading performance and distribution pattern of centrifugal variable-rate fertilizer applicator based on DEM software. Comput. Electron. Agric. 144, 249–259.
Kretz, D., Callau-Monje, S., Hitschler, M., Hien, A., Raedle, M., Hesser, J., 7]. Discrete element method (DEM) simulation and validation of a screw feeder system. Powder Technol. 287, 131–138.
Melanz, D., Fang, L., Jayakumar, P., Negrut, D., 8]. A comparison of numerical methods for solving multibody dynamics problems with frictional contact modeled via differential variational inequalities. Comput. Methods Appl. Mech. Eng. 320, 668–693.
Kirsch, S., 9]. Avoiding ambiguity in DEM in-situ calibration for dry bulk materials. Miner. Eng. 145, 94–106.
Mohajeri, M.J., van Rhee, C., Schott, D.L., 2021. Replicating stress-history dependent behaviour of cohesive solid materials: Feasibility and definiteness in DEM calibration procedure. Adv. Powder Technol. 32 (5). https://doi.org/10.1016/j.apt.2021.02.044.
Obermayr, M., Vrettos, C., Eberhard, P., Däuwel, T., 0]. A discrete element model and its experimental validation for the prediction of draft forces in cohesive soil. J. Terramech. 53, 93–104.
Edilbert, A., Spaargaren, R., Geijs, C., Ruijgrok, J., Lodewijks, G., Schott, D., 2019. Design of a High Speed Transfer Chute in a confined Space–A DEM Case Study.
Grima, A.P., Fraser, T., Hastie, D.B., Wypych, P.W., 2011. Discrete element modelling: trouble-shooting and optimisation tool for chute design, pp. 1–10.
Kessler, F., Prenner, M., 2009. DEM – Simulation of Conveyor Transfer Chutes, pp. 185–192.
Gao, W., Wang, J., Yin, S., Feng, Y.T., 4]. A coupled 3D isogeometric and discrete element approach for modeling interactions between structures and granular matters. Comput. Methods Appl. Mech. Eng. 354, 441–463.
Otto, H., Zimmermann, A., Kleiber, M., Katterfeld, A., 5]. Optimization of an orange peel grab for wood chips. Mech. Mech. Eng., 112–119
Lommen, S.W., Schott, D.L., Lodewijks, G., 6]. Multibody dynamics model of a scissors grab for co-simulation with discrete element method. FME Transactions 40 (4), 177–180.
Lommen, S., Lodewijks, G., Schott, D.L., 7]. Co-simulation framework of discrete element method and multibody dynamics models. Eng. Comput. 34, 1481–1499.
Mohajeri, M., van Rhee, C., Schott, D.L., 2018. Penetration resistance of cohesive iron ore: A DEM study. In: 9th International Conference on Conveying and Handling of Particulate Solids, no. September, pp. 1–7.
Ai, J., Chen, J., Rotter, J.M., Ooi, J.Y., 0]. Assessment of rolling resistance models in discrete element simulations. Powder Technol. 206 (3), 269–282.
Wensrich, C.M., Katterfeld, A., 1]. Rolling friction as a technique for modelling particle shape in DEM. Powder Technol. 217, 409–417.

Iwashita, K., Oda, M., 2]. Rolling resistance at contacts in simulation of shear band development by DEM. J. Eng. Mech. 124 (3), 285–292.
Lommen, S., Schott, D., Lodewijks, G., 3]. Particuology DEM speedup : Stiffness effects on behavior of bulk material. Particuology 12, 107–112.
Lommen, S., Mohajeri, M., Lodewijks, G., Schott, D., 4]. DEM particle upscaling for large-scale bulk handling equipment and material interaction. Powder Technol. 352, 273–282.
Lommen, S.W., 5]. Virtual prototyping of grabs: co-simulations of discrete element and rigid body models. Delft University of Technology, Delft.
Weisberg, S., 2005. Applied linear regression, vol. 528.